Pramāṇa – J. Phys., Vol. 31, No. 5, November 1988, pp. 365–381. © Printed in India.

Some aspects of laser-metal vapour interaction

B S YILBAŞ and Z YILBAŞ
Erciyes Üniversitesi, Mühendislik Fakültesi, Kayseri, TURKEY

MS received 22 April 1988

Abstract. The vapour beam interaction plays an important role in laser machining process, since the vapour generated on the workpiece surface absorbs some fraction of the incident beam and heats the workpiece surface. Consequently, a study of this interaction mechanism is essential. For this purpose, a computer program was developed to investigate the interaction interaction, it provides a foundation to do further studies. It was found that the vapour locally high pressure gradients. Although the analysis presents a simplified picture of the interaction, it provides a foundation to do further studies. It was found that the vapour temperature reaches 5000 K after 10^{-6} s for a laser pulse of 10^{11} W/m^2 power intensity. The leading edge of the vapour velocity had a velocity of the order of 4000–7000 m/s.

Keywords. Laser-metal vapour interaction; vapour velocity; radiation absorption; radiation emission; conductivity; free-electron density; finite difference approximation.

PACS No. 32·80

1. Introduction

The vapour/beam interaction presents two major problems. The first is to predict the effect of heating on the state of the vapour and its expansion. The second is to determine how changes in the vapour state affect the absorption properties and the attenuation of the laser beam. A computer program has been developed to investigate the interaction in the above surface region, close to the target surface where the vapour expansion is driven by locally high pressure gradients.

The program uses the one-dimensional form of equations of gas-dynamics in Lagrangian coordinates to govern the vapour expansion. Additional terms in the equations account for the absorption of laser beam energy, radiation losses and conduction. The vapour is presumed to comprise of heavy particles and free electrons, each species behaving as a perfect gas. Possible deviations of the free electron density from its Saha equilibrium value are discussed and approximations allowed for in the computer program.

Finally some numerical solutions for the expansion of vapour plugs for a range of initial conditions are presented. These solutions do not cover every possible situation as a result of the sensitivity of the solutions to changes in initial conditions; however some characteristics and trends are discernable and these are described.

2. Basic equations and approximations

The model is based on the one-dimensional equations of gas-dynamics. Lagrangian coordinates are used to facilitate the location of free boundary and because the spacing

of these coordinates expands with the vapour, avoiding the necessity of introducing additional coordinates in the later stages of expansion. In the following, X is the Eulerian space coordinate and x is the Lagrangian coordinate ($x = X$ at $t = 0$). In Lagrangian form the momentum and mass conservation equations are

$$\partial u/\partial t = -(1/\rho_i)(\partial P/\partial x) \tag{1}$$

$$V = (1/\rho_i)(\partial X/\partial x) \tag{2}$$

where V and ρ_i are the specific volume and the initial density respectively. The energy equation is

$$\partial E/\partial t = P\frac{\partial V}{\partial t} + (2\alpha I - R_L)V + \frac{K}{\rho_i^2 V}\left[\frac{\partial^2 T}{\partial x^2} - \frac{1}{V}\left(\frac{\partial T}{\partial x}\right)\left(\frac{\partial V}{\partial x}\right)\right], \tag{3}$$

where E is the specific internal energy per unit mass. R_L represents radiative losses per unit volume and $2\alpha I$ is the laser beam absorption per unit volume so the second group of terms on the right hand side of the equation is the net rate of absorption per unit mass. The symbol K represents thermal conductivity, the third group of terms resulting from heat conduction.

The velocity u is given by

$$w = \partial X/\partial t. \tag{4}$$

Power intensities used for drilling or machining operations are in general well below the critical power intensity $I_{\text{crit}} \gtrsim 10^{14}$ W/m^2 (Yilbas 1981) at which the free-electron temperature starts to diverge significantly from the heavy particle temperature. Consequently the particle species are taken to have the same temperature. Assuming each species behaves as a perfect gas the equation of state is

$$P = \rho RT(1 + \beta), \tag{5}$$

where β is the degree of ionization. The specific internal energy per unit mass (E) is related to the temperature T by:

$$E = \frac{1}{M}\left(\frac{3}{2}kT(1 + \beta) + \beta U\right), \tag{6}$$

where M is the mass per atom, U the ionization energy per atom and k the Boltzmann constant.

Equations (1)–(6) form a system of partial differential equations which govern the expansion of the vapour. Before a solution is possible, however, some additional relationships are required to determine the net rate of absorption of radiation, and the degree of ionization. The correct value of the free electron density is discussed later.

2.1 *Radiation absorption and emission*

The power radiated per unit volume due to bremsstrahlung and recombination emission is given by Griem (1964)

$$R_L = (64/3)(\pi/3)^{1/2}\frac{n^2 U^{3/2}(kT)^{1/2} n_i n_e}{c^3 m^3}(1 + 2U/kT), \tag{7}$$

where the Gaunt factors have been taken as unity. Substituting the numerical values,

$$R_L(\mathrm{W/m^3}) = 2{\cdot}83 \times 10^{-30} \times U^{3/2}(\mathrm{eV}) n_i(\mathrm{cm}^{-3}) n_e(\mathrm{cm}^{-3}) T^{1/2}(\mathrm{K}) \times (1 + 2310U(\mathrm{eV})/T(\mathrm{K})).$$

The effective attenuation coefficient, α, may be calculated from earlier results (Yilbas 1987), by summing the contributions due to electron neutral and electron-ion collisions and photoionization:

$$\alpha = \alpha_{en} + \alpha_{ei} + \alpha_p, \tag{8}$$

where from equation (3),

$$\alpha_{en} = \frac{w}{c}\left\{\frac{w^2 + v_{\mathrm{av}}^2 - w_p^2}{2(w^2 + v_{\mathrm{av}}^2)}\left[\left\{1 + \left(\frac{w_p^2 v_{\mathrm{av}}}{w(w^2 + v_{\mathrm{av}}^2 - w_p^2)}\right)^2\right\}^{1/2} - 1\right]\right\}^{1/2}, \tag{9}$$

where v_{av} is given by equation (11). On the other hand (Huges 1975)

$$\alpha_{ei} = \zeta_f \cdot \frac{32\pi^2}{6} \cdot \left(\frac{2\pi}{3mkT}\right)^{1/2} \cdot \left(\frac{e^2}{4\pi\varepsilon_0}\right) \cdot \frac{hUn_i n_e}{\mathrm{cm}^3 w^3}, \tag{10}$$

$$\alpha_p = \zeta_b \cdot \frac{16\pi kTn_n U}{6\sqrt{3}mcw^3 h^2}\left(\frac{e^2}{4\pi\varepsilon_0}\right)\exp(-U/kT) - 1. \tag{11}$$

Finally, the local instantaneous power intensity I_x may be calculated by determining the degree of attenuation of the beam on reaching the point of interest using the integral relationship.

$$I_x = I_\infty \exp \int_\infty^x -2\alpha \, \mathrm{d}X. \tag{12}$$

2.2 *Conductivity*

The thermal conductivity K is the sum of the conductivities for heavy particles and free electrons respectively:

$$K = K_n + K_e. \tag{13}$$

Lee *et al* (1973) reported that

$$K_n = \frac{25}{64} \cdot \frac{3k}{\pi a_0^2}\left(\frac{\pi kT}{M}\right)^{1/2} \tag{14}$$

where the collision cross-section has been taken to be πa_0^2 where a_0 is the Bohr's radius. Mitchner and Kruger (1973) reported that

$$K_e = \frac{2{\cdot}4}{1 + v_{ei}(\sqrt{2}(v_{ei} + v_{en})} \frac{k^2 n_e T}{m(v_{ei} + v_{en})}. \tag{15}$$

The electron-ion collision frequency is calculated using (10)

$$v_{ei} = w^2 2\alpha_{ei}/w_p^2 c. \tag{16}$$

The electron-neutral collision frequency is calculated as (Mitchner and Kruger, 1973)

$$\nu_{en} = \frac{8\pi^{1/2}}{3}(m/2kT)^{-1/2}a_0^2 n_n. \tag{17}$$

Only the free electron number density remains undetermined. Under steady state collision-dominated conditions, this will be computed using the Saha equation:

$$\frac{\beta^2}{1-\beta^2} = \frac{2g + (2\pi m)^{3/2}kT^{5/2}}{gPh^3(2\pi)^3}\exp(-U/kT), \tag{18}$$

where

$$\beta = n_e/(n_i + n_n). \tag{19}$$

The resulting value for the free electron density may be modified on two counts. Firstly, the relaxation time for the free electron density may be significant compared to the characteristic time for changes in the vapour state. Secondly, the free electron density may be depressed below its Saha equilibrium value if radiative recombination is significant. These effects are taken into account by using the simple approximations described below.

(i) *Relaxation time for free electron density*

The net rate of production of free electrons may, in principle, be determined from the rate equation for the process. When collisional processes dominate photoionization and photorecombination processes the rate equation reduces to the Saha equation and the atomic excited states have Boltzmann distribution under steady state conditions. Before steady state conditions are reached the rate equation is

$$\dot{n}_e = \dot{n}\text{ (collisional ionization)} - \dot{n}\text{(three body recombination)}$$

The collisional ionization term is of the form

$$\dot{n}_e = \textstyle\sum_i n_e n_{n_i} A_i, \tag{20}$$

where n_{n_i} is the density of atoms in the ith excited state and A_i is the cross-section for collisional ionization from the ith level. Consequently, for the case of an initially depressed free electron density, when the recombination term is small, the relaxation time for a steady state is given by

$$\tau = 1/(\textstyle\sum_i n_{n_i} A_i). \tag{21}$$

Equation (21) cannot be evaluated in general because of lack of information. An overestimate for τ is possible if it is assumed that the atoms are ionized as a result of electron transitions from the ground state. Using an order-of-magnitude value for A_i, (Zeldovich and Raizer 1966) τ is found to be

$$\tau \sim 10/n_n(\text{cm}^{-3}). \tag{22}$$

However, this estimate is reasonable only if the neutral atoms are in a ground state and if it is assumed that the free electron density would be effectively constant over the duration of a pulsed laser interaction lasting times $< 10^{-3}$ s. This possibility conflicts at least with the results of high power interaction studies which show that the electron

density may vary in times which are orders of magnitude smaller than τ. If, alternatively, the excited states have an equilibrium Boltzmann distribution the rate of ionization is greatly increased, since the ratio of excited atoms to ground state atoms in unit time is high. The ratio for hydrogen atoms is (Zeldovich and Raizer 1966);

$$\frac{\dot{n}_e\,(\text{excited atom contribution})}{\dot{n}_e\,(\text{ground atom contribution})} \quad \begin{matrix} i^6 \text{ from level} \\ \frac{2}{5}\left(\frac{U_H}{kT}\right) i^4 \text{ from high level.} \end{matrix} \tag{23}$$

The relaxation time is instantaneous if the excited states have a Boltzmann distribution (Yilbas, 1983); consequently the relaxation time for the free electron density is also the time to establish a Boltzmann distribution of atomic excited states. Assuming that an estimate of the time τ_β taken to establish a Boltzmann distribution given by Zeldovich and Raizer (1966)

$$\tau_\beta = \frac{1}{u n_e A} \sim \frac{10^{11}}{n_e(\text{cm}^{-3}) T^{1/2}(\text{K})}, \tag{24}$$

τ_β is plotted for a range of conditions of interest (figure 1). Putting $\tau = \tau_\beta$, the free electron density is determined from:

$$n_e = n_{e_{\text{initial}}} \cdot \exp(-t/\tau) + n_{e_{\text{equilibrium}}} \cdot (1 - \exp(-t/\tau)). \tag{25}$$

(ii) *Depression of free electron density due to radiative recombination*

The Saha equation (equation (18)) is valid when thermodynamic equilibrium is established. However, when the radiation losses from the vapour are significant the rate of radiative capture of free electrons may be sufficient to depress the steady state number density below its equilibrium value. The deviation from the Saha equation value is

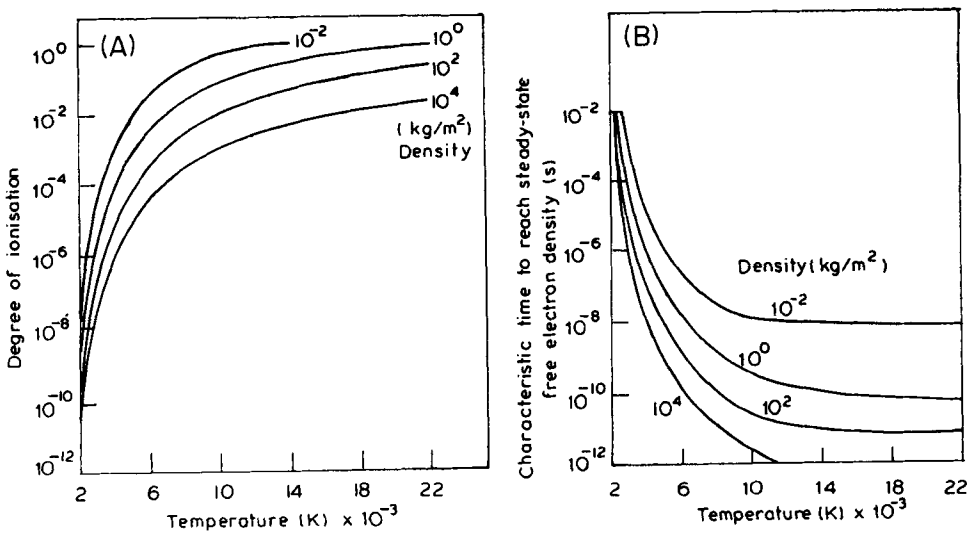

Figure 1. Degree of ionization and characteristic time for copper vapour.

significant when the rate of radiative capture of free electrons approaches or exceeds the rate of three-body recombination. The deviation is negligible when

$$\frac{\text{rate of three body collisional recombination}}{\text{rate of radiative capture}} \geqslant 1,$$

or

$$\left(\sum_i n_e c_{S_i} \Big/ \sum_i A_{ci}\right) > 1 \tag{26}$$

where c_{S_i} is the rate integral for collisional transitions and A_{ci} is the Einstein coefficient for radiative capture (Cherrington 1979). Considering only recombination into the ground state and using an order of magnitude values for c_{S_i} and A_{ci} given in Landau and Lifshitz (1960), equation (26) gives

$$n_e \geqslant \sim 10^{12}(\text{cm}^{-3})$$

for $T \sim 10^3$–10^4 K. Neglecting the deviations from a Boltzmann distribution of excited states, the free electron density is obtained from the rate equation to be

$$n_e(\text{cm}^{-3}) = \frac{10^{12}}{2}\left(1 + \frac{4n_{e_{\text{Saha}}}^2}{10^{24}}\right) - 1. \tag{27}$$

For the conditions of interest, the deviation from the Saha equilibrium value $n_{e_{\text{Saha}}}$ is negligible.

The corresponding degree of ionization of a range of conditions is given in figure 1 for copper.

3. Finite difference approximations

The finite difference approximations to the previously described gas-dynamic equations are as close as possible to those given by Richtmyer and Morton (1967).

The finite difference approximations to equations (1), (2), and (3) are, respectively

$$u_j^{n+1} = u_j^n - \frac{1}{\rho_i \Delta x}\left(P_{j+1/2}^n + P_{j-1/2}^n + q_{j+1/2}^n - q_{j-1/2}^n\right)\Delta t, \tag{28}$$

$$V_{j-1/2}^{n+1/2} = (X_j^{n+1} - X_{j-1}^{n+1})/\rho_i(x_j - x_{j-1}), \tag{29}$$

$$X_j^{n+1} = X_j^n + u_j^{n+1}\Delta t, \tag{30}$$

where j and n are the spatial and temporal coordinate numbers respectively, and $j^{+1/2}$ is the point midway between coordinates j and $j+1$.

In (28), q is an artificial damping term which allows stable computation through near discontinuites such as shock waves. q is defined by (Zeldovich and Raizer 1966)

$$q = \frac{\Gamma \Delta x^2}{V}\left(\frac{\partial u}{\partial x}\right)^2 \frac{\partial u}{\partial x} < 0, \tag{31}$$

$$q = 0 \quad (\partial u/\partial x) > 0, \tag{32}$$

where r is a constant factor typically taken to be 2 or 3. For $r = 2$,

$$q_j^n{}_{+1/2} = \frac{4}{V_j^n{}_{+1/2} + V_j^{n-1}{}_{+1/2}} [u_j^n{}_{+1} - u_j^n]^2 \quad \text{for} \quad u_j^n{}_{+1} - u_j^n < 1, \tag{33}$$

$$q_j^n{}_{+1} = 0 \quad \text{for} \quad u_j^n{}_{+1} - u_j^n \geqslant 0. \tag{34}$$

The energy equation (3) is approximated to

$$\begin{aligned} E_j^{n+1}{}_{-1/2} = E_j^n{}_{-1/2} &- \left(P_j^n{}_{-1/2} + q_j^{n+1}{}_{-1/2} \right) \left(V_j^{n+1}{}_{-1/2} - V_j^n{}_{-1/2} \right) \\ &+ \left(\alpha_j^n{}_{-1/2} I_j^n{}_{-1/2} - R^n_{L_j{}_{-1/2}} \right) \Delta t \left(V_j^{n+1}{}_{-1/2} + V_j^n{}_{-1/2} \right) \\ &+ \frac{K_j^n{}_{-1/2} \Delta t}{\Delta x^2 \rho_i^2 V_j^n{}_{-1/2}} \left(T_j^n{}_{+1/2} - 2T_j^n{}_{-1/2} + T_j^n{}_{-3/2} \right). \end{aligned} \tag{35}$$

The conduction term is approximated to the form which has a known stability criterion when conduction effects dominate the gas-dynamic motion.

To determine the intensity distribution in the vapour the absorption equation (12) is integrated from the free surface of the vapour using

$$I_j^n{}_{-1/2} = I_j^n{}_{+1/2} \cdot \exp\left[-(\alpha_j^n{}_{+1/2} + \alpha_j^n{}_{-1/2}) \cdot (X_j^n{}_{+1} - X_j^n{}_{-1})/2 \right]. \tag{36}$$

A complete stability analysis is prevented by the nonlinearity of the equations. Richtmyer and Morton (1967) investigated the stability of the system of equations (in which conduction and radiation absorption terms are dropped) after linearizing them. The analysis shows that the Courant number (C_0) should satisfy the inequality

$$C_0 < \sqrt{\gamma}/\Gamma^2, \tag{37}$$

where

$$C_0 = (\sqrt{\gamma P}/\rho) \cdot (\rho \Delta t / \rho_i \Delta x). \tag{38}$$

In the limit when conduction effects dominate the minimum requirement for the stability of the conduction equation is

$$(\lambda \Delta t / \Delta x^2) < \tfrac{1}{2} \tag{39}$$

where $\lambda = K/\rho C_p$ is the thermal diffusivity of the vapour.

The time increment Δt is determined by using the most restrictive of the inequalities (equations (37) or (39)).

4. Boundary conditions and order of solution of equations

The spatial coordinate numbers are $j = 1, 2, 3, \ldots, Y$. The coordinate $j = Y$ corresponds to the free surface of the expanding material. The coordinate $j = 1$ corresponds to a boundary plane in the material at which the velocity is known at all times and at which some assumption is necessary to allow for heat transfer to the target bulk.

Initially all material properties are known or may be calculated. The power intensity distribution through the domain of the coordinate system is calculated using (36):

$$I_j^{n-1/2} = I_j^{n+1/2} \cdot \exp\left[-(\alpha_j^{n+1/2} + \alpha_j^{n-1/2}) \cdot (X_j^{n+1} - X_j^{n-1})/2\right]$$

and incrementing backwards from $j = Y - 1,\ Y - 2, \ldots,\ 2$. For $j = Y$

$$I_Y^{n-1/2} = I_\infty^n \cdot \exp\left[-\alpha_Y^{n-1/2}(X_Y^n - X_{Y-1}^n)\right]. \tag{40}$$

After establishing the power intensity distribution, the vapour expansion over a period Δt is computed. The principal steps involved in solving the equations for values at time $t + \Delta t$ are as follows:

Equations (28) and (33) or (34) are used to compute u_j^{n+1}, starting from $j = 2, 3, \ldots, Y$. To compute u_j^{n+1} the required free boundary conditions are:

$$P_{Y+1/2}^n = 2P_a - P_{Y-1/2}^n, \tag{41}$$

where P_a is the ambient pressure (equal to zero for expansion into a vacuum), and also

$$q_{Y+1/2}^n = q_{Y-1/2}^n. \tag{42}$$

This latter condition cancels the effect of artificial damping at the free surface.

Equation (30) is used to compute X_j^{n+1}, and then equations (29) and (35) are used to compute $V_{j-1/2}^{n+1}$ and $E_{j-1/2}^{n+1}$, respectively, for $j = 2, 3, \ldots, Y$. Conduction losses at the free boundary are neglected and the boundary condition required to compute $E_{Y-1/2}^{n+1}$ is

$$T_{Y+1/2}^n = 2T_{Y-1/2}^n - T_{Y-3/2}^n. \tag{43}$$

Equation (6) is used to determine $T_{j-1/2}^{n+1}$:

$$T_{j-1/2}^{n+1} = \Phi_1(E_{j-1/2}^{n+1}, \beta_{j-1/2}^n) \tag{44}$$

Equations (7) and (18), (7) and (24), and (7) and (25) are used to determine $B_{j-1/2}^{n+1}$

$$\beta_{j-1/2}^{n+1} = \Phi_2(T_{j-1/2}^{n+1}, V_{j-1/2}^{n+1}). \tag{45}$$

Subsequently (5) is used to determine $P_{j-1/2}^{n+1}$

$$P_{j-1/2}^{n+1} = \Phi_3(T_{j+1/2}^{n+1}, V_{j-1/2}^{n+1}, \beta_{i-1/2}^{n+1}). \tag{46}$$

This sequence avoids iteration. If however, the degree of ionization changes significantly in Δt, (44) and (45) are solved simultaneously.

The computed field is advanced to a new time $t = t + \Delta t$. New values for material properties are now computed so that $\alpha_j^{n+1/2}$ ($\equiv \beta_{j-1/2}^{n+1}$ for the previous sequence) is available. The power intensity is recalculated using (36), thereby initiating a new step in time of length Δt.

5. Results and discussion

Numerical solutions for the expansion of these plugs are described in the following.

A number of variables require initial values which are only approximately estimated

or which may vary significantly in the range of conditions suitable for laser machining applications. These values may be systematically varied to provide a range of solutions with different possible initial conditions, but a large number of solutions are required before the deduction of laws governing the interaction becomes a possibility. This situation has not been reached in the period of this project. However the results described in the following serve to indicate some of the principal influences on the evolution of the vapour/laser beam interaction.

The computed results pertain to ND YAG laser light ($w = 1{\cdot}78 \times 10^{15}\,s^{-1}$). For the light of other frequencies the absorption coefficient will differ for the same vapour state, although changing the light frequency will have almost the same effect as changing the power intensity. The difference between the two is that changes are produced in the relative importance of components of the effective attenuation coefficient only by changing the light frequency.

The initial plug depth (D) and the initial vapour density (ρ_v) are related to the amount of material ejected per plug, which is deduced from experimental observations. The product $D\rho_v$ is a constant in the early period of the plug expansion if the expansion is assumed to be homogeneous but the correct value for D or ρ_v has to be determined using a further relationship. Since the most accurate results for the expansion are likely to be obtained by starting the solution as early as possible in the plug expansion the value of D closest to the plug depth before ejection is ideal. In practice D has to be larger than this value firstly so that the volume of the liquid ejected as part of the plug is small compared to the volume of the vapour and secondly in order to achieve a solution which extends over the desired period of the expansion in a reasonable computing time. Bearing in mind these considerations the initial plug depth D is estimated from (35)

$$D = 10d, \tag{47}$$

where d is the depth of the material ejected from the dense phase per plug and is typically 10–20 μm giving a value of D equal to between 100 and 200 μm.

Variations in D for a given density have the effect of reducing or increasing the time taken for the vapour expansion to propagate from the free surface through the vapour plug. Computed results show that vapour near the leading edge of the plug is most likely to produce a hot spot. In this case D is greater than the minimum value and its variation has less effect than that of other variables.

The initial density may be estimated from (36):

$$\rho_v = \rho_0(1 - g)/(10 - g), \tag{48}$$

where ρ_0 is the solid material density and g is the fraction of material ejected in liquid form. Using (48) the initial vapour density is estimated to be of the order 10^1–$10^2\,kg/m^3$.

Variations in initial density influence the interaction by changing the distribution within the vapour plug of energy absorption. As the initial plug density is increased the temperature increase due to heating by the laser beam becomes more localized, the hot spot occurring in the half of the plug nearest to the laser. This effect is apparent when figure 2 is compared to figure 3. Each figure gives solutions for the same initial conditions except for the initial density.

The initial proportion of the beam power dissipated in the vapour increases as the initial density increases. This does not necessarily result in more rapid increases in

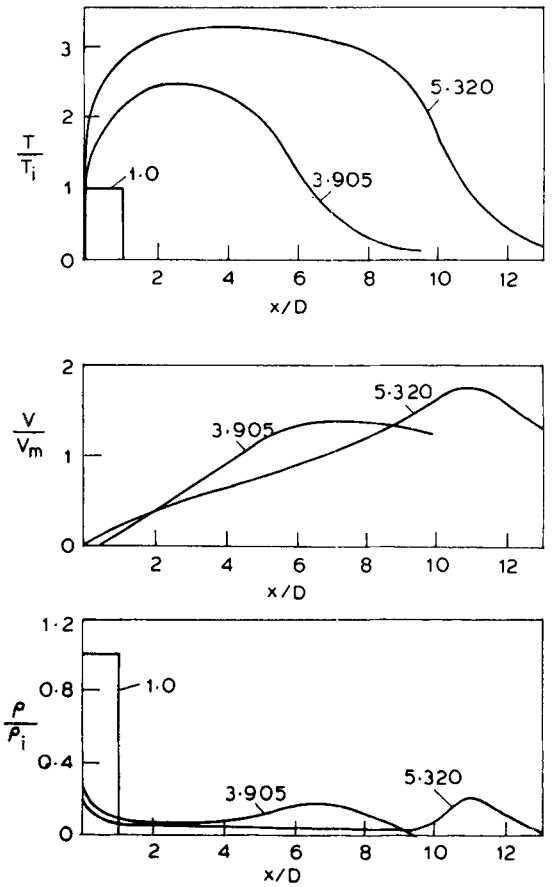

Figure 2. Plug expansion at t/τ for $T_i = 10000\,\text{K}$; $\rho_i = 10\,\text{kg/m}^3$; $D = 100\,\mu\text{m}$; $I = 1{\cdot}4 \times 10^{11}\,\text{W/m}^2$; $\tau = 0{\cdot}068\,\mu\text{s}$; $V_m = 2773\,\text{m/s}$; copper vapour.

temperature during the expansion for higher initial densities, and under some circumstances the vapour may cool. The absorbed energy per unit mass does not necessarily increase and since the absorbed energy is concentrated nearer the leading edge of the vapour than is the case for lower densities the energy may be converted from internal to kinetic energy more rapidly.

An order of magnitude estimate for the initial plug temperature is given by (8).

$$T(K) = 10^{-7} I(\text{W/m}^2). \tag{49}$$

This suggest that the initial plug temperature should be typically 10000 K.

To indicate the importance of the initial temperature, this was varied for a series of solutions for which other initial conditions were constant. The solutions for copper vapour are plotted in figures 2 and 4, for initial temperatures of 8000 and 10000 respectively. For an initial temperature of 8000 K the vapour plug cooled as it expanded whereas when the initial temperature was 10000 K or more the vapour temperature increased rapidly during the early stages of the expansion. The rate of increase of temperature was approximately the same for temperatures of 10000 K.

The sensitivity of the expansion to changes in initial temperature in the region of

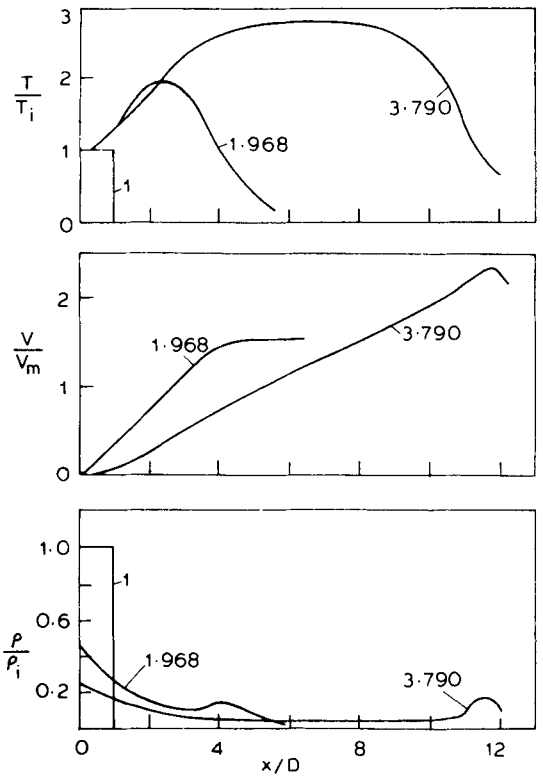

Figure 3. Plug expansion at t/τ for titanium vapour. Initial conditions: $\rho_i = 10\,\text{kg/m}^3$; $T_i = 10000\,\text{K}$; $D = 100\,\mu\text{m}$; $I = 1{\cdot}4 \times 10^{11}\,\text{W/m}^2$; $\tau = 0{\cdot}058\,\mu\text{s}$; $V_m = 3322\,\text{m/s}$.

10000 K is due to the rapid variation of the attenuation coefficient with temperature. The response of the vapour to beam absorption tends to reinforce the initial trend towards more or less absorption. For example if insufficient beam energy is absorbed to compensate for the energy radiated and convected to kinetic energy the vapour cools, becomes more transparent and subsequently cools more rapidly.

Increasing the power intensity does not necessarily lead to an increased rate of temperature rise throughout the plug. The increase may produce a response similar to that for increases in density, namely a hot spot may be generated near the leading edge of the vapour. This feature is illustrated in figure 5 which shows the effect of increasing the power intensity incident on the vapour from $1{\cdot}4 \times 10^{11}$ to $5 \times 10^{11}\,\text{W/m}^2$. Whereas the low power intensity was insufficient to produce a temperature rise in the vapour, which subsequently became rapidly transparent, the higher power intensity produced a rapid rise in temperature near the leading edge of the vapour.

Because of significant differences between experimental results for respective metals (Yilbas 1983), it is relevant to determine how sensitive the results are to target material changes.

Figures 2 and 3 present results for the expansion of different metal vapours (Ta, Ni, Cu, Fe) under the same initial conditions. The variation of peak temperature with time is shown for each metal in figure 6.

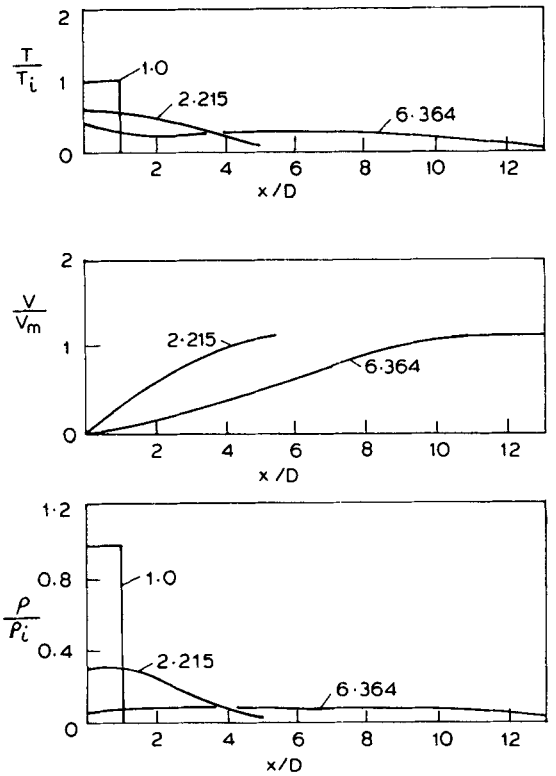

Figure 4. Plug expansion at t/τ for $T_i = 80000$ K. Initial conditions: $\rho_i = 10\,\text{kg/m}^3$; $D = 100\,\mu\text{m}$; $I = 1{\cdot}4 \times 10^{11}\,\text{W/m}^2$; $\tau = 0{\cdot}075\,\mu\text{s}$; $V_m = 2400\,\text{m/s}$, copper vapour.

These results show that the variation of peak temperature and the features of the expansion are similar for each metal when the initial conditions are the same, although the beam attenuation in the vapour varied by more than a factor of two between metals as shown in figure 7. This indicates that the initial conditions for each metal vapour expansion influence the expansion form and these initial conditions will be significantly different for each metal.

When the initial conditions were such that the vapour temperature increases with time during the expansion two types of expansion were observed. For low initial densities and power intensities as in figure 2, for example ($10\,\text{kg/m}^3$, $1{\cdot}4 \times 10^{11}\,\text{W/m}^2$), the vapour is heated uniformly and the temperature increase is similar for the bulk of the vapour. When either the density or the power intensity is increased a hot spot occurs in the plug. As a result, the heating and expansion of vapour on the target side of the hot spot is restricted and the plug may be effectively split into two parts. This effect, which may restrict the ejection of target material to discrete bursts, is apparent in figure 8 for which the initial density was $100\,\text{kg/m}^3$ and the power intensity was $1{\cdot}4 \times 10^{11}\,\text{W/m}^2$.

Near the leading edge of the vapour the density is higher than in the middle section of the plug, typically by a factor of two or more, as a result of the velocity gradient decreasing in the region of the leading edge.

The vapour state changes rapidly in the early stages of the expansion but by the time the plug has expanded to a height of between 1 and 2 mm the rate of change has slowed.

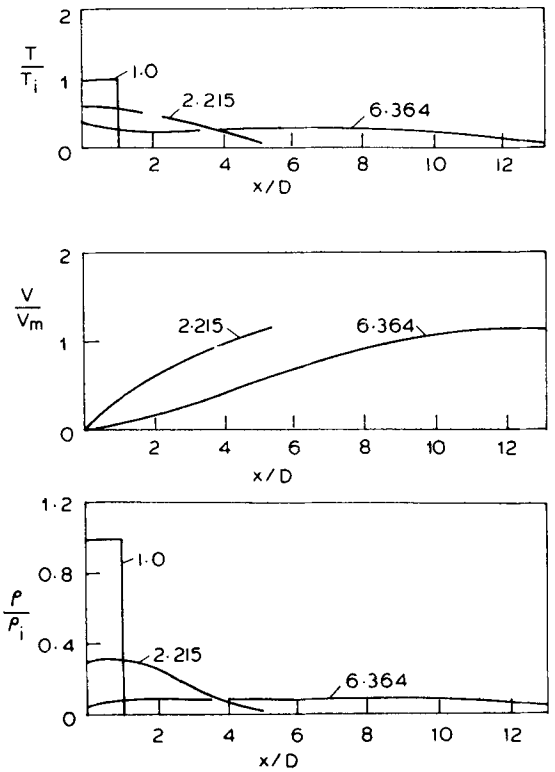

Figure 5. Plug expansion at t/τ for copper vapour. Initial conditions: $\rho_i = 10\,\text{kg/m}^3$; $T_i = 8000\,\text{K}$; $D = 100\,\mu\text{m}$; $I = 1{\cdot}4 \times 10^{11}\,\text{W/m}^2$; $\tau = 0{\cdot}075\,\mu\text{s}$; $V_m = 2400\,\text{m/s}$, copper vapour.

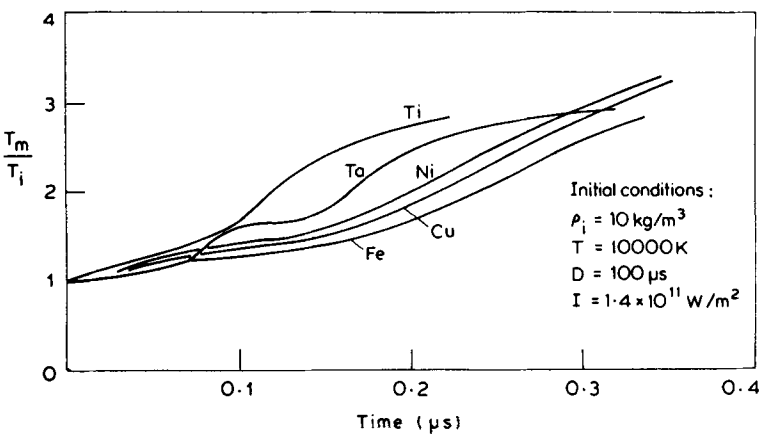

Figure 6. Variation of instantaneous maximum temperature (T_m) for a range of metals.

In the later stages of the expansion a large proportion by volume of the plug has a characteristic temperature and density which for the results plotted are between 30000 and 50000 K and of the order 10^0 kg/m^3 respectively. Initial pressures are typically 10^3 bar dropping to values of the order of 10^1 bar during the first microsecond of the

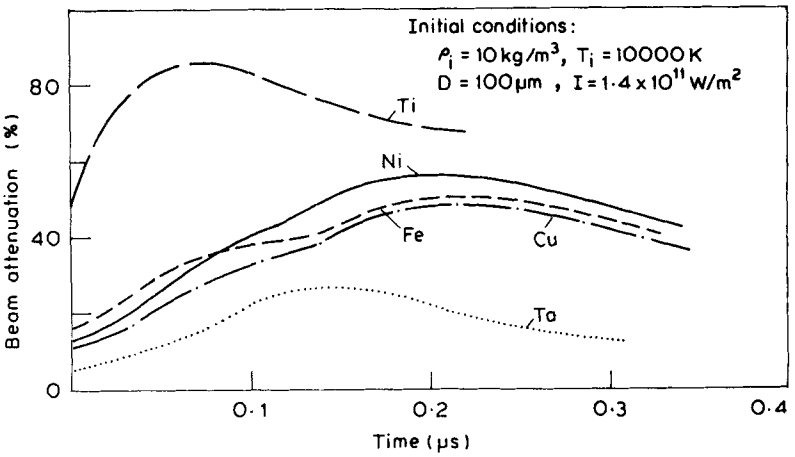

Figure 7. Beam attenuation at the surface for a range of metals.

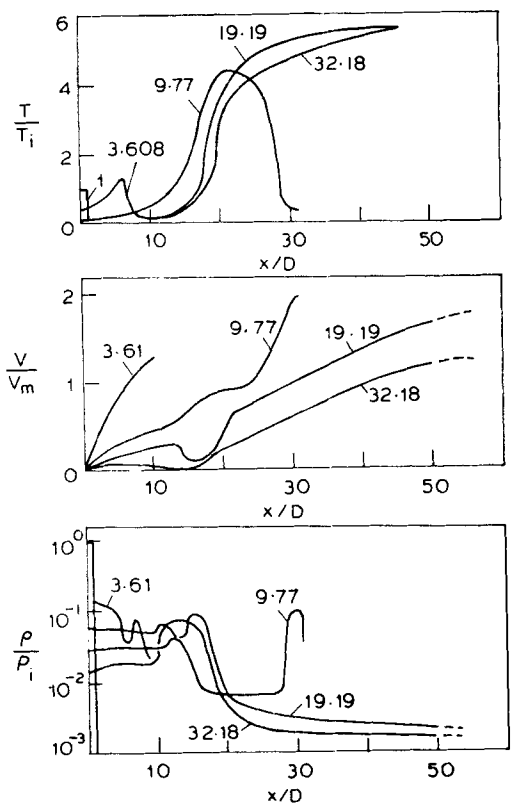

Figure 8. Plug expansion at t/τ for $\rho_i = 100\,\text{kg/m}^3$; Initial conditions; $T_i = 10000\,\text{K}$; $D = 100\,\mu\text{m}$; $I = 1{\cdot}4 \times 10^{11}\,\text{W/m}^2$; $\tau = 0{\cdot}059\,\mu\text{s}$; $V_m = 3961\,\text{m/s}$, titanium vapour.

expansion. The degree of ionization depends on the temperature and the density and consequently varies considerably. The initial degree of ionization is typically about 5%, for the computed results. This value may increase to 100% in hot spots or decrease to a fraction of 1% during an axpansion.

The vapour velocity reaches a maximum near the leading edge of the vapour. This maximum value increases as the expansion proceeds but at a decreasing rate. The value is typically between $(3/2)x$ and $2x$, the maximum velocity for an isotropic vapour expansion from the same initial conditions, producing a leading edge velocity of 4000–7000 m/s. This prediction does not appear unreasonable in the light of experimental observations. The expansion rate of flares is too high to be deduced from streak photographs on which times of the order of 10 μs may be resolved, suggesting the leading edge velocity is at least 10^3 m/s.

The vapour thermal conductivity determined using equation (13) is typically 10^1 W/mK. This value is orders of magnitude less than the conductivity of solid metals ($K = 400$ W/mK for solid copper) and so the importance of conduction in the vapour is far less than in the solid.

The rate at which heat is transferred to the target by conduction is dependent on the initial conditions for the expansion since, for example, the vapour adjacent to the surface may be sufficiently screened for the local temperature to actually drop below the initial temperature as in figure 8. Of the solutions presented, that given in figure 2 has the greatest temperature gradient at the surface. The corresponding rate of heat transfer to the target at 0·3 μs after the beginning of the expansion, is of the order 10^7 W/m^2. This is negligible compared to the power deposited on the surface by the transmitted part of the beam, namely $1{\cdot}2 \times 10^{11}$ W/m^2, indicating that the influence of conduction at the surface is small.

The power loss due to radiation emission is typically at least an order of magnitude less than the power absorbed from the laser beam for the combinations of initial conditions considered. Consequently these losses do not lead to a significant reduction in vapour temperature unless the laser beam is strongly attenuated in the leading section of the vapour. When this occurs the vapour close to the surface may suffer a net heat loss which leads to a temperature drop.

Below the power intensity for which radiation losses exceed the power absorbed, the vapour temperature will inevitably drop during the expansion. For drilling or machining conditions using a ND YAG laser, the critical power intensity below which there is a net radiation loss from plasma is about $10^9 - 10^{10}$ W/m^2.

The percentage attenuation of the laser beam in the vapour varies over a wide range during the vapour expansion and when the initial conditions for the expansion are changed. Some indication of the variation is given by figures 7 and 9, which give the percentage attenuation as a function of time for a range of initial temperatures and metals respectively. The initial density and plug dimension and the incident power intensity were the same for each result, namely $\rho = 10$ kg/m^3, $D = 100\,\mu$m, $I = 1{\cdot}4 \times 10^{11}$ W/m^2. The peak attenuations for these results were between 27% and 87%. Figure 7 shows that the expansions for similar initial conditions for different metals produce dissimilar beam attenuation variations. However before these results may be fully interpreted, the variation of the initial conditions between metals must be determined more fully. The instantaneous reduction in power for copper vapour is shown as a function of distance in figure 5 where the total instantaneous attenuation is the value for $x/D = 0$.

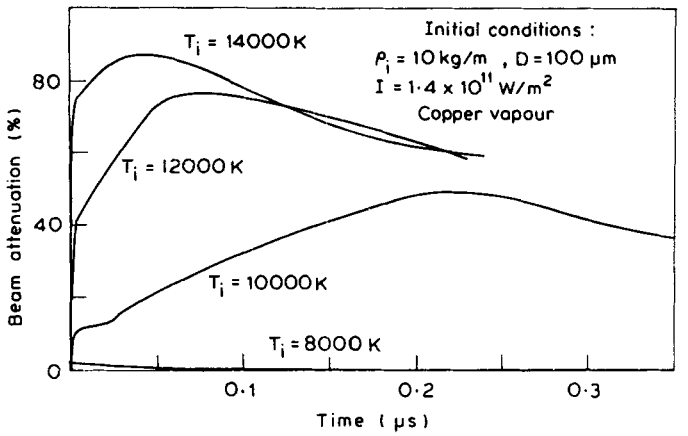

Figure 9. Beam attenuation at the surface for a range of initial temperatures.

For solutions when a higher initial density was used as in figure 8 (when ρ_v was 100 kg/m^3) the peak attenuation was greater and the power intensity was reduced by a maximum of three orders of magnitude by absorption by the vapour.

These results complement the experimental results which show the power intensity of the machining laser will be strongly attenuated by the vapour ejecta. The computed 1·06 μm wavelength radiation absorption depth varies over the range 10^{-2}–10^{-5} m, but is typically 10^{-3} m. This is compatible with the observed absorption depths of 10^{-3} m for helium-neon laser light (6348 A wavelength).

6. Conclusion

Numerical solutions for the beam/vapour interaction show that the evolution of the expansion of a vapour plug is sensitive to variations in initial conditions.

For a laser light wavelength of 1·06 μm and an incident power intensity of about 10^{11} W/m^2 on the vapour, the vapour temperature increases from initial values of approximately 10000 K to 30000–50000 K in 10^{-7}–10^{-6} seconds after which further increases occur relatively slowly. The vapour density drops from 10^1–10^2 kg/m^3 to typically 10^0 kg/m^3 for the bulk (by volume) of the plug during the same period. The leading edge of the vapour has a velocity of the order of 4000–7000 m/s.

References

Cherrington B E 1979 *Gaseous electronics and gas lasers* (London: Pergamon)

Griem H R 1964 *Plasma spectroscopy* (New York: McGraw Hill)

Hughes T P 1975 *Plasmas and laser light* (London: Adam Hilger)

Landau L D and Lifshitz E M 1960 *Electrodynamics of continuous media* (trans. by J B Sykes and J S Bell) *Course of theoretical physics* (Oxford: Oxford Press Ltd.) Vol. 8

Lee J F, Sears F W and Turcotte D L 1973 *Statistical thermodynamics* (London: Addison-Wesley) 2nd ed.

Mitchner M and Kruger C H 1973 *Partially ionised gases* (New York: Wiley Interscience)

Richtmyer R D and Morton K W 1967 *Difference methods for initial value problems* (*Tracts in pure and applied mathematics*) (New York: Interscience) 2nd ed., No. 4

Yilbas B S 1981 *Heat transfer mechanisms initiating the laser drilling of metals*, Ph.D thesis, Birmingham University, UK

Yilbas B S 1983 *Statistical thermodynamics*, Lecture notes, Erciyes University, Kayseri, Turkey

Yilbas B S 1987 *Propagation of a laser beam through atmosphere—A design consideration for laser beam machine* IE(I) Journal PR, **68** 9

Zeldovich Y B and Raizer Y P 1966 *Physics of shock waves and high temperature hydrodynamic phenomena* (eds) R F Probstein and W O Hayes (New York: Dover Publishing Ltd.)